

ORIGINAL ARTICLE

CRF receptor type 2 neurons in the posterior bed nucleus of the stria terminalis critically contribute to stress recovery

MJAG Henckens^{1,2}, Y Printz¹, U Shamgar¹, J Dine², M Lebow^{1,2}, Y Drori^{1,2}, C Kuehne², A Kolarz², M Eder², JM Deussing², NJ Justice³, O Yizhar¹ and A Chen^{1,2}

The bed nucleus of the stria terminalis (BNST) is critical in mediating states of anxiety, and its dysfunction has been linked to stress-related mental disease. Although the anxiety-related role of distinct subregions of the anterior BNST was recently reported, little is known about the contribution of the posterior BNST (pBNST) to the behavioral and neuroendocrine responses to stress. Previously, we observed abnormal expression of corticotropin-releasing factor receptor type 2 (CRFR2) to be associated with post-traumatic stress disorder (PTSD)-like symptoms. Here, we found that CRFR2-expressing neurons within the pBNST send dense inhibitory projections to other stress-related brain regions (for example, the locus coeruleus, medial amygdala and paraventricular nucleus), implicating a prominent role of these neurons in orchestrating the neuroendocrine, autonomic and behavioral response to stressful situations. Local CRFR2 activation by urocortin 3 depolarized the cells, increased the neuronal input resistance and increased firing of action potentials, indicating an enhanced excitability. Furthermore, we showed that CRFR2-expressing neurons within the pBNST are critically involved in the modulation of the behavioral and neuroendocrine response to stress. Optogenetic activation of CRFR2 neurons in the pBNST decreased anxiety, attenuated the neuroendocrine stress response, ameliorated stress-induced anxiety and impaired the fear memory for the stressful event. Moreover, activation following trauma exposure reduced the susceptibility for PTSD-like symptoms. Optogenetic inhibition of pBNST CRFR2 neurons yielded opposite effects. These data indicate the relevance of pBNST activity for adaptive stress recovery.

Molecular Psychiatry advance online publication, 23 August 2016; doi:10.1038/mp.2016.133

INTRODUCTION

The bed nucleus of the stria terminalis (BNST) is a unique processing junction in the brain. Its dense connectivity pattern places it at the center of the brain's emotional processing network.^{1–4} It is a physical hub linking numerous distant regions, connecting input from limbic forebrain structures to hypothalamic and brain stem regions associated with autonomic and neuroendocrine systems to mediate a plethora of behavioral functions. Although the BNST has historically received rather limited attention, evidence is beginning to accumulate for its critical role in the mediation of the neuroendocrine stress response⁵ and anxiety (for example, sustained fear);⁶ both being hallmarks of stress-related psychopathology. Notably, the BNST is a very heterogeneous conglomerate of subnuclei, which serve various functions through their diversity in cellular sub-populations and input and projection sites.^{3,4,7–10} In particular, the anterior and posterior sections of the BNST serve opposing roles in the mediation of the hypothalamus–pituitary–adrenal (HPA) axis. Whereas the anterior section has been implicated in the activation of the HPA axis to cause corticosterone release, the posterior BNST (pBNST) is known to send GABAergic projections to the paraventricular nucleus and thereby thought to inhibit HPA axis activation.^{5,11} Interestingly, corticotropin-releasing factor receptor type 2 (CRFR2) is highly expressed in the pBNST.¹² CRFR2 signaling has been implicated in the regulation of anxiety and the stress response, and has a critical role in stress recovery. Developmental

knockout animals for CRFR2^{13–15} or its primary ligands (urocortin (Ucn) 1–3)¹⁶ display an anxiogenic phenotype, increased corticosterone responses to stress and impaired stress recovery. Interestingly, recent studies have revealed a critical role for CRFR2 signaling specifically in the pBNST in the development of post-traumatic stress disorder (PTSD). Trauma-exposed animals that were susceptible to PTSD were characterized by abnormal CRFR2 expression levels in the BNST compared with their resilient littermates, and normalization of these levels significantly attenuated their PTSD-like phenotype.^{17,18} Here, we studied the specific contribution of these pBNST CRFR2-expressing neurons to anxiety-like behavior, the neuroendocrine and behavioral stress response, and PTSD susceptibility.

MATERIALS AND METHODS

Generation of CRFR2-cherry-2A-Cre-recombinase BAC

Engineering of the CRFR2-cherry-2A-Cre-recombinase (CRFR2-chy-Cre) bacterial artificial chromosome (BAC) was performed similar to as described in Liu *et al.*¹⁹ CRFR2-chy-f2a-Cre BAC DNA was purified (QIAGEN, Hilden, Germany) before being injected into single-celled mouse oocytes to generate transgenic mouse lines.

Animal background and maintenance

The CRFR2-Cre BAC transgene was maintained on a C57BL/6J (Harlan, Jerusalem, Israel) background. For all behavioral experiments, hemizygous

¹Department of Neurobiology, Weizmann Institute of Science, Rehovot, Israel; ²Department of Stress Neurobiology and Neurogenetics, Max Planck Institute of Psychiatry, Munich, Germany and ³Center for Metabolic and Degenerative Diseases, Institute of Molecular Medicine, University of Texas Health Sciences Center, Houston, TX, USA. Correspondence: Professor A Chen, Department of Neurobiology, Weizmann Institute of Science, Hertzl Street No. 234, Rehovot 7610001, Israel or Department of Stress Neurobiology and Neurogenetics, Max Planck Institute of Psychiatry, Kraepelinstraße 2-10, 80804 Munich, Germany. E-mail: alon.chen@weizmann.ac.il or alon_chen@psych.mpg.de

Received 19 November 2015; revised 24 May 2016; accepted 1 June 2016

CRFR2-Cre transgenic males were bred to channelrhodopsin (ChR2) (Ai32 mice, B6;129S-Gt(ROSA)26Sor^{tm32.1(CAG-COP4*H134R/eYFP)Hze/J}), Jackson Laboratory, Bar Harbor, ME, USA) or halorhodopsin (eNpHR3.0) (Ai39, B6;129S-Gt(ROSA)26Sor^{tm39(CAG-hop/eYFP)Hze/J}), Jackson Laboratory) conditional females. Only ChR2/eNpHR3.0-heterozygote male offspring was used for behavioral testing. Mice expressing the Cre-recombinase enzyme served as the experimental test group, and their littermates that did not, served as controls. All experiments were approved by the Institutional Animal Care and Use Committee of the Weizmann Institute of Science.

Stereotactic surgery

Anterograde tracing. Projection sites of pBNST CRFR2-expressing neurons were identified by unilateral injection of 0.3 μ l AAV5-EF1 α -DIO-eYFP (UNC Vector Core, Chapel Hill, NC, USA) into the pBNST of adult male CRFR2-Cre mice. The targeted injection site was 0.1 mm more ventral than for fiber-optic cannula placement to reach the center of the pBNST, on coordinates (relative to Bregma): AP -0.22, ML 1.60, DV -3.90.

Fiber-optic placement. Two fiber-optic cannulas (Doric Lenses, Québec, QC, Canada, DRC-MFC_200/260/900FLT, 200 μ m thick, 4 mm long) were inserted under an angle of \pm 10 degrees targeting Bregma coordinates: AP -0.22, ML \pm 1.60, DV -3.80,¹⁷ which defined the most dorsal part of the pBNST to allow light penetration to the entire region.

In vitro electrophysiological recording

Ligand infusion. Slices were continuously superfused (4–5 ml min⁻¹) with oxygenated artificial cerebrospinal fluid (in mM: 125 NaCl, 2.5 KCl, 1.25 NaH₂PO₄, 25 NaHCO₃, 1 MgCl₂, 2 CaCl₂ and 25 D-glucose, pH 7.3), containing 50 μ M APV, 5 μ M NBQX, 10 μ M bicuculline methiodide and 5 μ M CGP 55845. Borosilicate glass pipettes (Harvard Apparatus, Kent, UK) with resistances ranging from 4 to 5 M Ω were filled with intracellular solution (in mM: 130 K-gluconate, 5 NaCl, 2 MgCl₂, 5 D-glucose, 10 HEPES, 0.5 EGTA, 2 MgATP, 0.3 Na-GTP, 20 phosphocreatine, pH 7.3 with KOH). CRFR2-pBNST cells were identified by tdTomato expression. Electrophysiological measurements under control conditions were carried out 5 min after reaching the whole-cell configuration. The input resistance was calculated from steady-state voltage responses upon negative current injections (1500 ms) where no ‘sag’ could be detected. Firing frequency was evaluated by positive current injections (400 ms) that induced mild firing (1–4 action potentials (APs)) of the neurons under control conditions. Ucn3 (100 nM, Bachem, Bubendorf, Switzerland) was bath-applied and electrophysiological measurements were repeated 10 min after starting Ucn3 administration.

Photostimulation. The recording chamber was perfused with oxygenated artificial cerebrospinal fluid (in mM: 3 KCl, 11 glucose, 123 NaCl, 26 NaHCO₃, 1.25 NaH₂PO₄, 1 MgCl₂, 2 CaCl₂; 300 mOsm kg⁻¹) at a rate of \sim 2 ml min⁻¹ and maintained at 31–33 °C. Borosilicate glass pipettes (Sutter Instrument, Novato, CA, USA) with resistances ranging from 3 to 6 M Ω were filled with intracellular solution (in mM: 135 K-gluconate, 4 KCl, 2 NaCl, 10 HEPES, 4 EGTA, 4 MgATP, 0.3 NaTRIS; 280 mOsm kg⁻¹, pH 7.3 with KOH). Opsin-expressing pBNST cells were identified by eYFP expression. Whole-cell patch-clamp recordings were carried out using a Multiclamp 700B amplifier (Axon Instruments/Molecular Devices, Sunnyvale, CA, USA). Optical activation of ChR2 and eNpHR3.0 was performed using 475/28 nm and 586/20 nm light (Lumencor Spectra X, Beaverton, OR, USA), respectively, delivered through the microscope illumination path.

In vivo optogenetic control of neuronal activity

At the time of testing, two fiber-optic patchcords were connected to the fiber-optic cannulas and at the other end via FC/PC to a 1x2i intensity division fiber-optic rotary joint (Doric Lenses) that was suspended above the test arenas. The rotary joint was FC connected to the light source (either blue 473 nm-laser, or yellow/green 561 nm-laser, Crystalaser, Reno, NV, USA) which was located outside the testing room and controlled by a pulse generator (Agilent 33220A 20 MHz Waveform Generator, Agilent Technologies, Santa Clara, CA, USA). A light power of \sim 100 mW mm⁻² at the end of the fiber tip was used for photostimulation, providing a sufficient amount of light power density for opsin activation to a depth of \sim 0.8 mm from the tip.²⁰ For activation of ChR2, light trains at 20 Hz, with a 10 ms pulse-width of 473 nm light were used, whereas eNpHR3.0 was activated by constant illumination with 561 nm light.

Behavioral assessment

All behavioral testing was performed during the animals’ active phase (that is, dark cycle). Just before each behavioral test, fiber-optic cables were attached to the mouse’s head in a new cage. The animal was allowed to briefly recover before it was placed in the test apparatus. Testing was performed by an experimenter blind to the animals’ genotype, and behavioral output measures subjected to statistical testing were generated by automated analyses unless specified otherwise. Randomization was not used as the animals’ genotype determined their allocation to the corresponding experimental group.

Statistics

All statistical analyses were performed using SPSS software (IBM Software, Armonk, NY, USA). Student’s *T*-tests (independent samples, two-tailed) were used to determine group differences during periods of photostimulation, whereas a repeated-measures analysis of variance was used in the behavioral tests in which effects of photostimulation were repeatedly measured (that is, marble burying and tail suspension test). Paired samples *T*-tests were used for comparisons within animals (that is, for *c-Fos* expression and electrophysiology data). One-tailed tests were only used in case of a clear hypothesis on the directionality of the results (that is, for the electrophysiology and PTSD phenotype).¹⁷ For all *T*-tests, a Levene’s test for equality of variances was performed and if significant, *T*-values and degrees of freedom were reported based on *T*-tests not assuming equal variance. Non-parametric Spearman’s correlations were used to determine the correlation between the electrophysiological measures of spiking success rate and the photocurrent amplitude, whereas Barnard’s test²¹ was used to assess differential distribution of PTSD phenotype between experimental groups. Bonferroni correction was applied in case of multiple comparisons. Alpha was set at 0.05 throughout. Data points deviating $>$ 2 s.d. from the mean were considered outliers and excluded from analyses.

RESULTS

Inhibitory pBNST CRFR2 neurons are densely connected to stress-related brain nuclei and excited by Ucn3

To study the nature and exact function of CRFR2-expressing neurons in the pBNST, we generated a novel BAC transgenic mouse line expressing Cre-recombinase under the control of the brain-selective alpha-splice variant of the *Crf2* gene. Several mouse lines were generated, and screened for Cre-recombinase expression by crossbreeding them with tdTomato reporter mice (Ai9, B6.Cg-Gt(ROSA)26Sor^{tm9(CAG-tdTomato)Hze/J}). tdTomato expression was subsequently verified in brain regions known to express CRFR2, that is, the olfactory bulb, lateral septal nucleus, ventromedial hypothalamic nucleus, medial and posterior cortical nuclei of the amygdala, ventral hippocampus, mesencephalic raphe nuclei and the pBNST.¹² The transgenic mouse line showing the highest Cre-recombinase expression in the majority of these regions (Supplementary Figure 1), and importantly, very high expression levels in the pBNST (Figure 1a, Supplementary Figure 2), was selected for further testing.

The vast majority of the pBNST neurons expressing CRFR2 are GABAergic in nature as demonstrated by two independent findings. First, conditional mutagenesis data showed that the conditional knockout of CRFR2 in GABAergic neurons specifically, in CRFR2^{GABA-CKO} mice, completely depleted CRFR2 in the pBNST (Figure 1b, Supplementary Figure 3). Second, double *in situ* hybridization data for tdTomato—as expressed in the pBNST CRFR2-Cre⁺ neurons—and GABAergic neuronal markers, GAD65-/67, revealed a high degree of colocalization (\sim 80% (232/301 neurons)), indicating the pBNST CRFR2 neurons are GABAergic (Figure 1c).

Next, we examined the projection targets of pBNST CRFR2 neurons by injecting Cre-dependent AAV5-EF1 α -DIO-eYFP into the pBNST of our CRFR2-Cre mouse line, labeling all axons of local CRFR2 neurons by eYFP expression. Specificity of transduction was validated by the presence of eYFP-positive neuronal cell bodies solely in the pBNST. In line with previous findings on projection

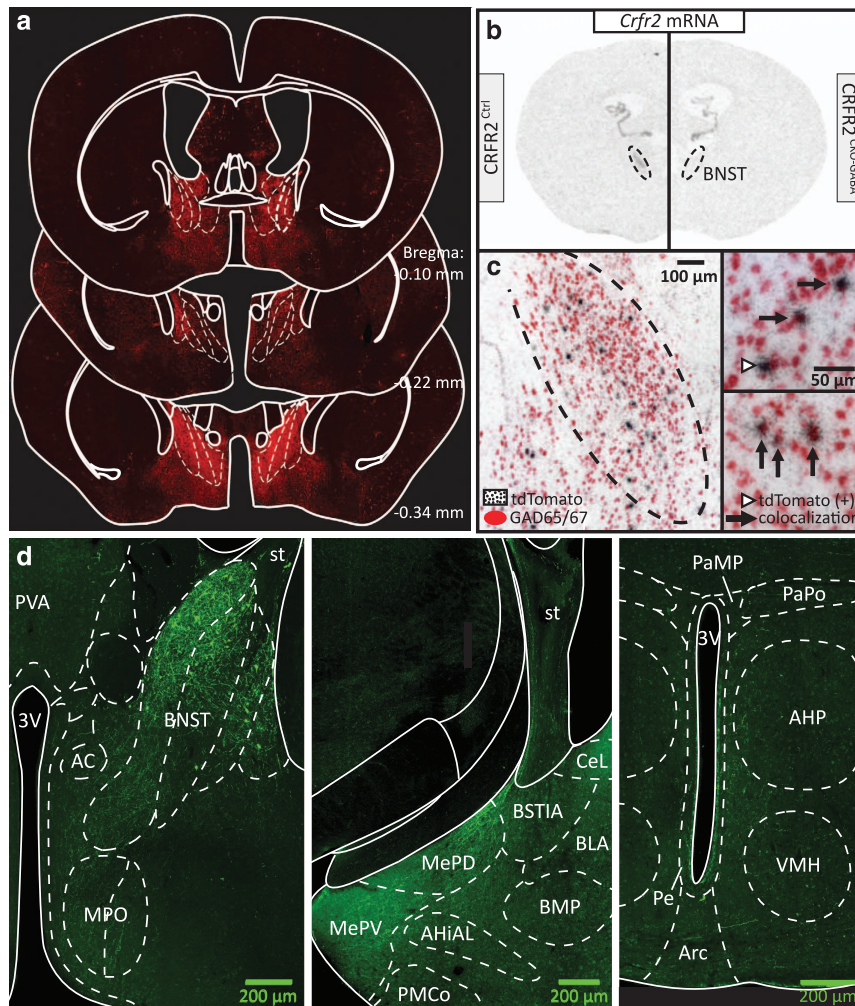


Figure 1. Characterization of posterior bed nucleus of the stria terminalis (pBNST) corticotropin-releasing factor receptor type 2 (CRFR2)-expressing neurons in CRFR2-Cre mice. **(a)** Coronal brain sections of CRFR2-tdTomato⁺ mice showing strong tdTomato expression in the pBNST. **(b)** Expression analyses of CRFR2 mRNA in the pBNST of a wild-type (CRFR2^{ctrl}) and GABAergic CRFR2 conditional knockout mouse line (CRFR2^{GABA-CRKO}). **(c)** Double *in situ* hybridization of tdTomato (silver grains), and GAD65/67 mRNA (red staining) in the posterior BNST (Bregma -0.22 mm) of the CRFR2-tdTomato⁺ mouse brain. Filled arrows indicate cells coexpressing tdTomato and GAD65/67, whereas arrow heads depict cells positive for tdTomato expression only. **(d)** Projection sites of the pBNST CRFR2-expressing neurons as identified using Cre-dependent AAV5-EF1 α -DIO-eYFP (see also Supplementary Figure 4). Key: third ventricle (3V); anterior commissural nucleus (AC); amygdalohippocampal area, anterolateral part (AHiAL); anterior hypothalamic area, posterior part (AHP); arcuate hypothalamic nucleus (Arc); basolateral amygdaloid nucleus, anterior part (BLA); basomedial amygdaloid nucleus, posterior part (BMP); bed nucleus of the stria terminalis intraamygdaloid division (BSTIA); central amygdaloid nucleus, lateral division (CeL); medial amygdaloid nucleus, posterodorsal part (MePD), posterodorsal part (MePV); median preoptic area (MPO); paraventricular hypothalamic nucleus, medial parvocellular part (PaMP), and posterior part (PaPo); periventricular hypothalamic nucleus (Pe); posteromedial cortical amygdaloid nucleus (PMCo); paraventricular thalamic nucleus, anterior part (PVA); stria terminalis (st); ventromedial hypothalamic nucleus (VMH).

sites of the pBNST as a whole,⁸ we observed dense projections to several nuclei of the hypothalamus (median preoptic area, paraventricular nucleus, arcuate nucleus and ventromedial hypothalamus), and through the stria terminalis to the medial amygdala (Figure 1d). Projections were also observed in the paraventricular thalamic nucleus, lateral septum and two brain stem nuclei; the locus coeruleus and periaqueductal gray (Figure 1d, Supplementary Figure 4). This projection pattern implies a prominent role for pBNST CRFR2-expressing neurons in orchestrating an appropriate neuroendocrine, autonomic and behavioral response to stressful situations.

Subsequently, we identified the probable endogenous ligand for CRFR2 in these neurons. Immunostaining for CRF, Ucn1 and Ucn3, showed the highest concentration of Ucn3 in the pBNST, whereas little CRF and no Ucn1 expression was observed

(Figure 2a, Supplementary Figure 5). This finding is in line with previous literature,²² and points to Ucn3 as the primary endogenous ligand for the pBNST CRFR2 neurons. To better understand the interaction between Ucn3 and CRFR2 in the pBNST, we next performed patch-clamp recordings in acute pBNST slices from CRFR2-tdTomato⁺ mice. We found that 6 out of 8 stably recorded (≥ 30 min) CRFR2-expressing neurons exhibited a pronounced 'sag' upon hyperpolarizing current injections and rebound firing after cessation of the current injections (Figure 2b, thinner line). Upon depolarizing current injections, these neurons responded in most cases with an initial 'burst' of spikes followed by a more regular firing pattern (Figure 2b, thicker line). Under blockade of ionotropic glutamate and GABA receptors, bath application of Ucn3 (100 nM) depolarized the neurons (Figure 2c, $T_{(7)} = 9.98$, $P < 0.001$). This effect was accompanied by

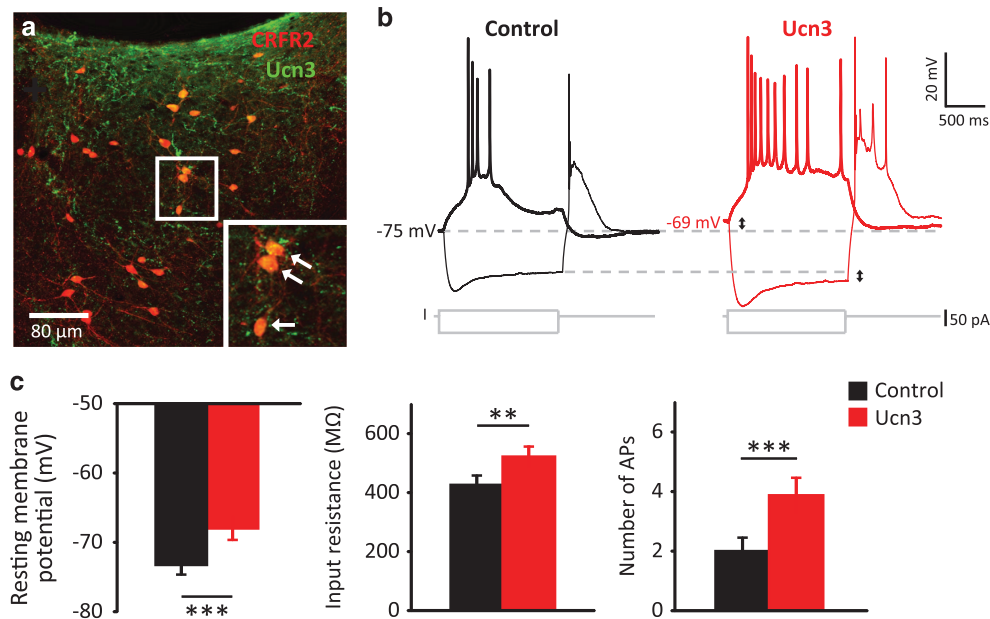


Figure 2. Effects of ligand (urocortin 3) application on posterior bed nucleus of the stria terminalis (pBNST) corticotropin-releasing factor receptor type 2 (CRFR2)-expressing neurons. **(a)** Immunohistochemistry in pBNST sections of CRFR2-tdTomato⁺ mice identified Ucn3 as endogenous ligand for CRFR2. Inset shows selected section in x2 magnification. **(b)** Representative traces of a recorded neuron under control conditions (black traces) and 10 min after bath application of Ucn3 (100 nM, red traces). Ucn3 caused a depolarization of the cell, an increase in the neuronal input resistance and an increased firing of action potentials (APs). Thinner lines represent the membrane potential deflections in response to a hyperpolarizing current injection, and the thicker lines the membrane response to a depolarizing current injection. **(c)** Quantification of Ucn3 effects on CRFR2-expressing neurons in the pBNST. Ucn3 induced a depolarization of the resting membrane potential, an increase in the input resistance and an increase in AP firing of CRFR2-expressing neurons ($n=8$). Error bars indicate s.e.m. $**P < 0.01$, $***P < 0.001$.

an increase in the neuronal input resistance ($P=0.008$, rank sum test). Consistent with the resultant enhanced excitability, we further found that the neurons fired more APs in response to positive current injections following Ucn3 application ($T_{(7)}=6.35$, $P < 0.001$).

Activation of pBNST CRFR2 neurons reduces anxiety and boosts stress recovery

To examine the specific role of pBNST CRFR2-expressing neurons in stress and anxiety, we next crossbred these CRFR2-Cre mice with channelrhodopsin (ChR2) conditional mice (Ai32 mice, B6;129 S-Gt(ROSA)26Sor^{tm32.1(CAG-COP4*H134R/YFP)Hze/J}). *In vitro* electrophysiological recordings were used to verify the activation of pBNST CRFR2-expressing neurons by blue light stimulation. We first measured the steady-state photocurrent in ChR2-eYFP-expressing cells using wide-field illumination with different blue light power densities (Figure 3a). Photocurrent amplitudes saturated at $\sim 11.6 \text{ mW mm}^{-2}$, and we therefore used this light power density in the following experiments. We next recorded the response of the cells to 10 ms light pulses delivered at 5, 10, 20 and 30 Hz, and measured the probability of spiking in response to individual pulses (success rate; Figure 3a). At 20 Hz, the stimulation frequency used in our subsequent *in vivo* experiments, the success rate was $> 60\%$, but varied between cells, including between cells recorded from the same mouse. We suspected that this variability arises from weaker photocurrents because of low expression of ChR2 in a certain population of CRFR2-positive neurons. Indeed, spiking probability showed a typical sigmoidal dependence on photocurrent amplitude (Supplementary Figure 6, $r=0.99$), suggesting that in cells with smaller photocurrents the depolarizing current was not sufficient to evoke APs. Next, to study the effects of photoactivation of pBNST CRFR2 neurons *in vivo*, CRFR2-ChR2 mice were implanted with fiber-optic cannulas into the

pBNST bilaterally for local light delivery (Figure 3b). Effectiveness and specificity of photostimulation *in vivo* was validated in CRFR2-ChR2 mice by quantifying activity-dependent immediate early gene (*c-Fos*) expression to track neuronal activation. Unilateral photostimulation significantly increased *c-Fos* expression in CRFR2-expressing neurons of the stimulated vs unstimulated side of the pBNST ($T_{(6)}=3.54$, $P=0.012$), whereas neighboring areas (for example, the lateral septum) did not show such lateral differences in expression (Supplementary Figure 7). To investigate the functional role of pBNST CRFR2-expressing neurons in anxiety, we probed freely moving mice under optogenetic control in two well-validated anxiety assays: the elevated plus maze (EPM) and the open field (OF) test, which are both based on a rodents' aversion to open spaces. To test whether anxiety-related behavior is modulated by pBNST CRFR2-expressing neuronal activation, we tested mice during periods of photostimulation and compared mice sensitive (that is, CRFR2-ChR2⁺) with those insensitive (that is, control; CRFR2-ChR2⁻) to illumination. Photoactivation of pBNST CRFR2-expressing neurons increased open-arm time ($T_{(15)}=3.03$, $P=0.008$) and the distance traveled in the open arms ($T_{(15)}=3.19$, $P=0.014$) of the EPM (Figure 3c). In the OF test, photostimulation increased the time spent in the center ($T_{(25)}=3.10$, $P=0.005$) and the distance traveled in the center (at trend level, $T_{(17)}=1.99$, $P=0.063$) (Figure 3d), without affecting general locomotion ($T_{(18)}=1.65$, $P=0.117$, Supplementary Figure 8a). In the absence of light, no significant differences were detected (all P 's > 0.05). No effects of photoactivation were observed in either compulsivity, as measured by the marble burying test (main effect of photoactivation, $F_{(1,25)} < 1$; time x photoactivation, $F_{(2,50)} < 1$, Supplementary Figure 8b), or depressive-like behavior, as assessed by the tail suspension test (main effect of photoactivation, $F_{(1,15)} < 1$; time x photoactivation, $F_{(5,75)} < 1$, Supplementary Figure 8c). Thus, selective activation of pBNST CRFR2-expressing neurons produced an acute anxiolytic effect.

We continued by testing the role of pBNST CRFR2-expressing neurons in mediating stress responsiveness and subsequent recovery. To ascertain the temporal role of pBNST CRFR2-

expressing neurons in the modulation of the HPA axis response to stress, and the time frame in which modulation of their activity is thus most effective, mice were exposed to an acute stressor and

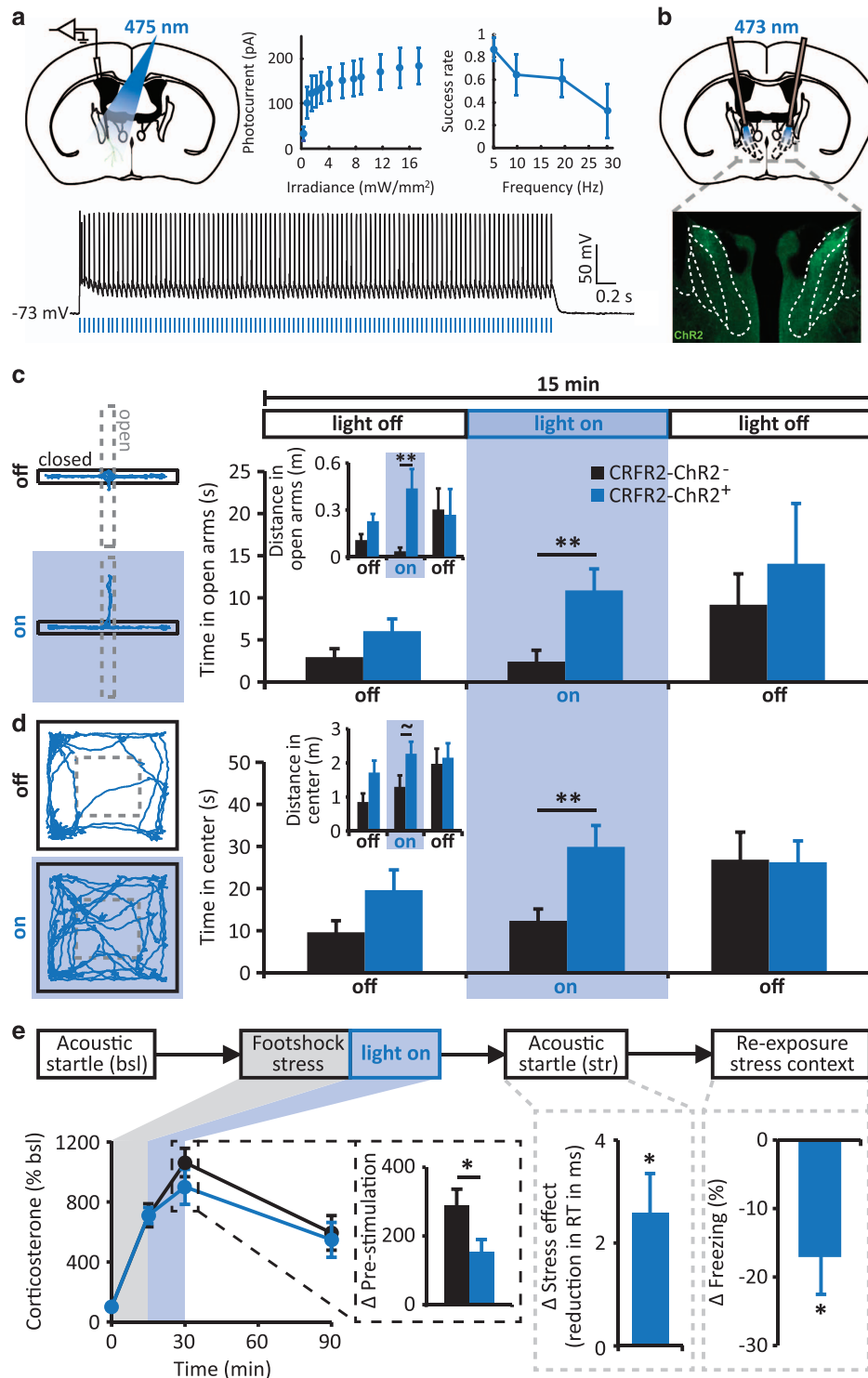


Figure 3. Effects of activating posterior bed nucleus of the stria terminalis (pBNST) corticotropin-releasing factor receptor type 2 (CRFR2)-expressing neurons. **(a)** Photostimulation of pBNST CRFR2-ChR2⁺ neurons *in vitro* induced reliable firing of recorded neurons, with >60% ($n=9$) success rate at 20 Hz stimulation. Steady-state photocurrent amplitude increased under increasing light intensities ($n=7-8$ for each intensity). **(b)** Mice were bilaterally implanted with fiber-optic cannulas into the pBNST to stimulate CRFR2-ChR2-expressing cells and subjected to behavioral tests. **(c, d)** Photostimulation reduced anxiety-like behavior in the elevated plus maze ($n_{\text{cre}+}=8$, $n_{\text{cre}-}=9$) and the open field test ($n_{\text{cre}+}=9$, $n_{\text{cre}-}=10$). **(e)** Photostimulation immediately following acute stress exposure reduced the stress-induced corticosterone response ($n_{\text{cre}+}=14$, $n_{\text{cre}-}=14$), reduced stress-induced anxiety ($n_{\text{cre}+}=9$, $n_{\text{cre}-}=9$), and attenuated memory for the stress context ($n_{\text{cre}+}=9$, $n_{\text{cre}-}=10$). Error bars indicate s.e.m. $\sim P < 0.1$, $*P < 0.05$, $**P < 0.01$.

received photostimulation either during the stress, immediately after, or with a 30-min delay. Photostimulation immediately following stress reduced the stress-induced increase in corticosterone levels ($T_{(8)}=2.24$, $P=0.042$, Supplementary Figure 9b), whereas stimulation at other time points was ineffective in modulating the neuroendocrine stress response (both $T_{(8)} < 1$, Supplementary Figures 9a and c). Therefore, we used this immediate recovery period for further investigation of the modulation of stress recovery in terms of stress-induced anxiety and memory of the stressful event by pBNST CRFR2 neurons. Mice were exposed to 15-min inescapable foot shock stress followed by 15-min photostimulation (Figure 3e), while we monitored their corticosterone response. Stress-induced anxiety was tested 1 day later by means of acoustic startle (that is, the defensive response to sudden or threatening stimuli, known to be modulated by fear),²³ which was compared with their 'baseline' startle response assessed 2 weeks earlier. Photoactivation of pBNST CRFR2-expressing neurons immediately following stress exposure again reduced the corticosterone stress response ($T_{(19.1)}=2.45$, $P=0.024$, Figure 3e), and also attenuated stress-induced anxiety ($T_{(16)}=2.52$, $P=0.023$, Figure 3e). The stress-induced shortening of the latency to peak startle, as indicative of hypervigilance,^{17,24} that was observed in the control animals (CRFR2-ChR2⁻, $F_{(1,8)}=30.38$, $P=0.001$), was prevented by activation of pBNST CRFR2-expressing neurons (CRFR2-ChR2⁺, $F_{(1,8)} < 1$). Moreover, activation of pBNST CRFR2-expressing neurons immediately following stress exposure reduced freezing behavior upon re-exposure to the stress context 6 weeks later ($T_{(9.3)}=2.57$, $P=0.030$, Figure 3e), which indicates a reduction in fear memory because of photostimulation. Altogether, these data indicate that activation of pBNST CRFR2-expressing neurons reduces anxiety and contributes to stress recovery by attenuating the neuroendocrine stress response, ameliorating stress-induced anxiety and attenuating the memory of the stressful event.

Inhibition of pBNST CRFR2 neurons increases anxiety and impairs stress recovery

Next, we wanted to test whether activation of pBNST CRFR2-expressing neurons occurs intrinsically when coping with stressful situations and is normally required for adaptive stress recovery. Therefore, we crossed the CRFR2-Cre mice with halorhodopsin (eNpHR3.0) conditional mice (Ai39, B6;129S-Gt (ROSA)26Sor^{tm39(CAG-hop/EYFP)Hze/J}) to allow for optogenetic inhibition of pBNST CRFR2-expressing neurons specifically. *In vitro* electrophysiological recordings were used to verify our ability to inhibit the activity of pBNST CRFR2-expressing neurons using photostimulation (Figure 4a). These recordings showed that depolarization of the neurons by injection of a step-current, induced robust spiking, which was reliably reduced (at 100 pA injection: $T_{(3)}=3.93$, $P=0.015$) or blocked entirely (at 50 pA injection: $T_{(3)}=3.71$, $P=0.017$) when activating eNpHR3.0 with yellow light. eNpHR3.0-mediated photocurrent amplitudes were 114.97 ± 16.53 pA (mean \pm s.e.m., $n=10$ cells) at peak and 29.88 ± 4.36 pA at steady state under 20.3 mW mm⁻² yellow light.

To examine the effect of photoinhibition of the pBNST CRFR2-expressing neurons on anxiety-like behavior, we implanted bilateral fiber-optic cannulas into the pBNST (Figure 4b) and subjected the mice to the EPM and OF tests, while they were exposed to periods of light delivery through the implanted optical fiber. Photoinhibition of pBNST CRFR2-expressing neurons reduced open-arm time ($T_{(15.4)}=2.62$, $P=0.019$) and distance traveled in the open arms ($T_{(21)}=2.34$, $P=0.029$) in the EPM (Figure 4c). It also decreased time spent in the center ($T_{(19)}=2.27$, $P=0.035$) and distance traveled in the center ($T_{(19)}=2.61$, $P=0.022$) in the OF test (Figure 4d), without affecting general locomotion ($T_{(11.7)}=1.62$, $P=0.132$, Supplementary Figure 8a). Although no differences between animals were observed during

initial exposure to these tests in the absence of photostimulation (all P 's > 0.05), in the OF test the effect of photoinhibition persisted into the last time bin (without stimulation), producing a longer-lasting state of (sustained) anxiety (time spent in the center, $T_{(19)}=2.70$, $P=0.014$; distance traveled in the center, $T_{(18)}=2.64$, $P=0.017$). Again, no effects of photoinhibition were observed in the marble burying test (main effect of photoinhibition, $F_{(1,22)} < 1$; time \times photoinhibition, $F_{(2,44)}=2.14$, $P=0.129$, Supplementary Figure 8b) or tail suspension test (main effect of photoinhibition, $F_{(1,20)} < 1$; time \times photoinhibition, $F_{(5,100)} < 1$, Supplementary Figure 8c). Thus, selective inhibition of pBNST CRFR2-expressing neurons produced an anxiogenic effect.

We continued by testing the intrinsic contribution of pBNST CRFR2 neuronal activity to stress recovery, using the same paradigm as described above, in which 15-min stress exposure was followed by 15 min of eNpHR3.0-mediated photoinhibition (Figure 3e). Although inhibition of pBNST CRFR2 neuronal activity did not have an immediate effect on the corticosterone response to stress ($T_{(22)} < 1$), we noted that it delayed stress recovery as measured by HPA axis normalization following stress, although this effect failed to reach significance after correction for multiple testing ($T_{(22)}=2.03$, $P_{corr}=0.110$, Figure 4e). In line with this observation, inhibition of pBNST CRFR2 neurons increased stress-induced anxiety in terms of acoustic startle (measured as latency to peak startle, $T_{(21)}=2.43$, $P=0.024$, Figure 4e), and enhanced fear memory for the stress context (as assessed by freezing upon re-exposure, $T_{(13.0)}=3.05$, $P=0.009$, Figure 4e). Thus, activity of pBNST CRFR2-expressing neurons seems to naturally contribute to coping with stressful situations and recovery from acute stress exposure. Compromised pBNST CRFR2 neuronal activity may therefore be a risk factor for stress-related psychopathology.

Activation of pBNST CRFR2 neurons reduces susceptibility to PTSD
Inadequate stress recovery is one of the key features of PTSD.²⁵ As altered CRFR2 expression in the pBNST was shown to contribute to a PTSD-like phenotype in rodents,^{17,18} we speculated that pBNST CRFR2 neuronal activity is critical for proper recovery from trauma exposure. To test this hypothesis, we first assessed overall pBNST activity levels in a PTSD-like model. To induce a PTSD-like phenotype, wild-type mice were exposed to a trauma (14 foot shocks (1 mA) in context A) followed by a trigger the next day (5 foot shocks (0.7 mA) in a different context B), and tested in a batch of behavioral tests assessing critical PTSD features: hypervigilance, insomnia, compulsivity and impaired risk assessment,¹⁷ in order to categorize the animals as either PTSD-like or resilient (Supplementary Figure 10). Next, pBNST immediate early gene mRNA expression levels, indicative of neuronal activation, were quantified and compared between groups. Indeed, the PTSD-like phenotype was associated with reduced neuronal activity of the pBNST (*Arc*: $T_{(12)}=2.49$, $P=0.028$, *c-Fos*: $T_{(13)}=2.52$, $P=0.025$, *Egr1*: $T_{(11)}=2.42$, $P=0.034$, *Npas4*: $T_{(11)}=2.81$, $P=0.017$, Figure 5a). This finding, together with the observation that pBNST CRFR2 neuronal activation contributes to stress recovery, suggests that increasing the activity of pBNST CRFR2 neurons following the PTSD induction protocol may enhance recovery and reduce susceptibility to develop PTSD. Thus, mice ($n_{\text{CRFR2-ChR2}^+}=12$, $n_{\text{CRFR2-ChR2}^-}=12$) were exposed to the trauma, and the next day received photostimulation immediately following the trigger (Figure 5b, upper panel). One week later, mice were behaviorally phenotyped and categorized as PTSD-like or resilient. PTSD-like mice showed significantly impaired risk assessment ($T_{(7)}=3.71$, $P=0.004$), a reduced latency to peak startle (indicative of hypervigilance, $T_{(12)}=2.47$, $P=0.015$), impaired prepulse-inhibition ($T_{(12)}=2.70$, $P=0.010$) and increased light activity (related to insomnia, $T_{(12)}=2.26$, $P=0.022$), compared with the resilient mice (Figure 5b, lower panel). Compulsive behavior was not significantly different between groups (number of marbles

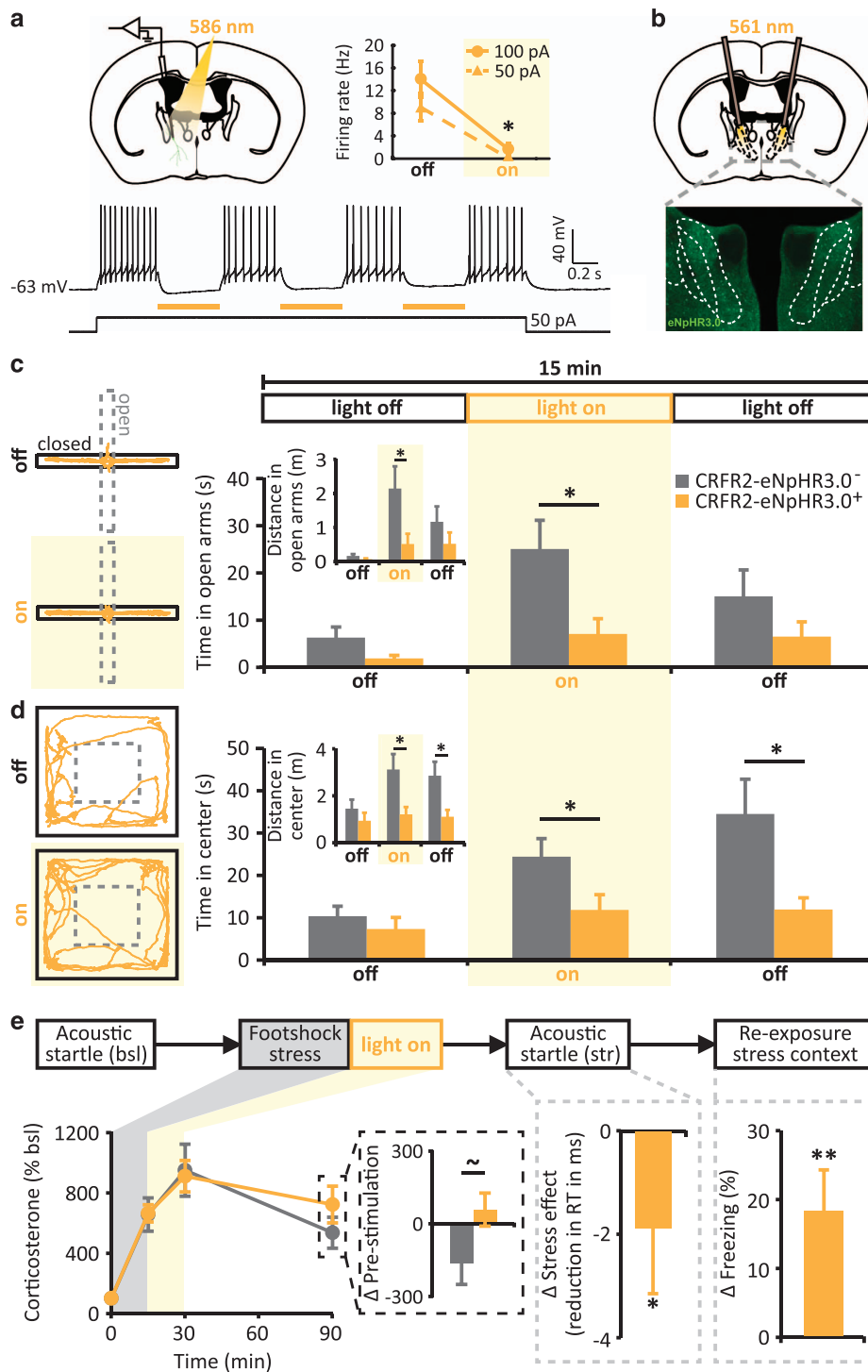


Figure 4. Effects of inhibition of posterior bed nucleus of the stria terminalis (pBNST) corticotropin-releasing factor receptor type 2 (CRFR2)-expressing neuronal activity. **(a)** Illumination with yellow light reliably suppressed the firing of pBNST CRFR2-eNpHR3.0⁺ neurons *in vitro* ($n=4$). **(b)** Mice were bilaterally implanted with fiber-optic cannulas into the pBNST to illuminate CRFR2-eNpHR3.0 cells and subjected to behavioral tests. **(c, d)** Photoinhibition increased anxiety-like behavior in the elevated plus maze ($n_{cre+}=12$, $n_{cre-}=11$) and the open field test ($n_{cre+}=11$, $n_{cre-}=10$). **(e)** Photoinhibition immediately following acute stress exposure tended to impair stress recovery in terms of the corticosterone response, increased stress-induced anxiety, and augmented memory for the stress context ($n_{cre+}=11$, $n_{cre-}=12-13$). Error bars indicate s.e.m. $\sim P_{corr}=0.11$, $*P < 0.05$, $**P < 0.01$.

buried, $T_{(12)} < 1$). Critically, we next checked the percentage of PTSD-like mice among those receiving activation of pBNST CRFR2-expressing neurons (CRFR2-ChR2⁺ mice), and those that did not (that is, CRFR2-ChR2⁻ mice, insensitive to photostimulation). Only

8% of the mice in which the pBNST CRFR2 neurons were activated following the trigger developed PTSD-like behavior, compared with 42% of the control mice (Figure 5c), indicating that activation significantly reduced susceptibility to PTSD development

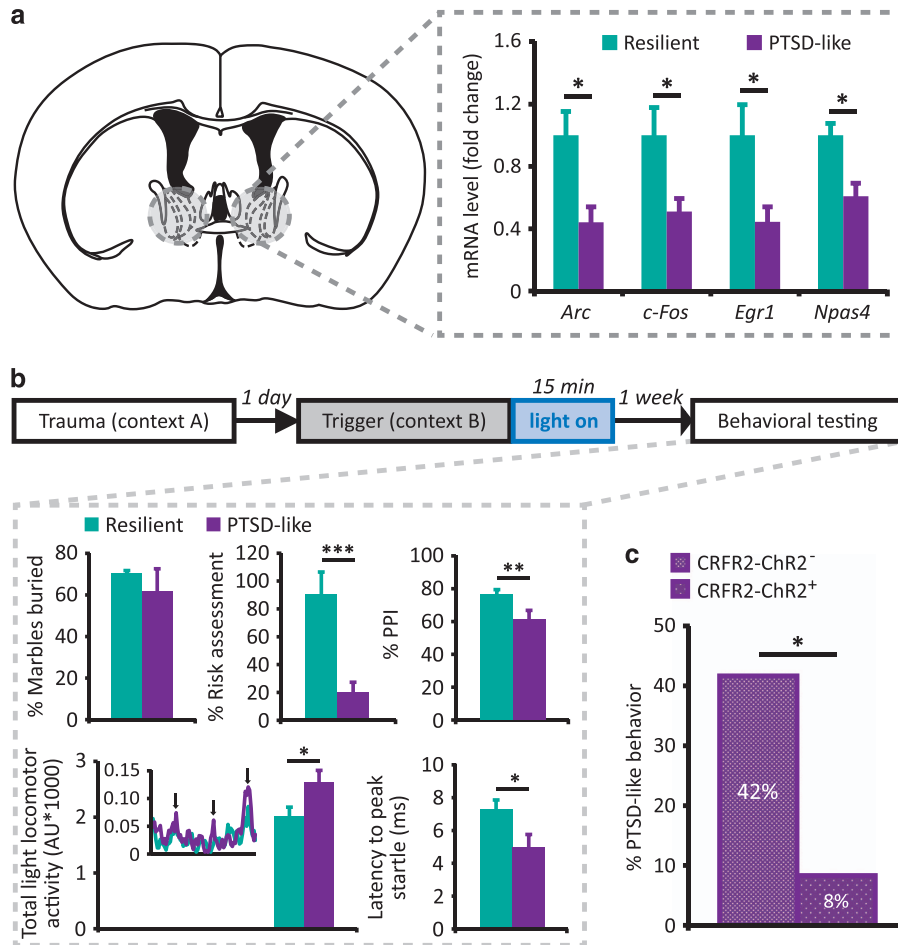


Figure 5. Involvement of posterior bed nucleus of the stria terminalis (pBNST) corticotropin-releasing factor receptor type 2 (CRFR2) neurons in PTSD. **(a)** PTSD-like animals showed reduced pBNST activity (that is, immediate early gene expression) compared with resilient animals ($n_{res}=6$, $n_{PTSD}=7$). **(b)** The PTSD induction protocol caused a PTSD-like phenotype in a subset of animals ($n_{PTSD}=6$), whereas others were resilient ($n_{res}=8$). **(c)** Activation of pBNST CRFR2 neurons immediately following PTSD induction reduced PTSD incidence ($n_{Cre+}=12$, $n_{Cre-}=12$). Error bars indicate s.e.m. * $p < 0.05$, ** $p < 0.01$, *** $p < 0.005$. PTSD, post-traumatic stress disorder.

($P=0.041$). Thus, these data indicate the relevance of the inhibitory tone by pBNST CRFR2 neuronal signaling for adequate stress recovery.

DISCUSSION

Previous studies have demonstrated anxiogenic and anxiolytic effects of activation of distinct subregions within the anterior BNST.^{26,27} Here we show that a specific sub-population of cells within the pBNST (that is, CRFR2-expressing neurons) is critically involved in the modulation of behavioral and neuroendocrine responses to stressful situations and subsequent recovery. Activity of these cells was associated with a robust anxiolytic phenotype. It induced an immediate reduction in basal anxiety, whereas activation in the immediate aftermath of stress attenuated corticosterone release, ameliorated stress-induced anxiety and attenuated memory of the stressful event. These effects are very likely mediated by the observed dense inhibitory projections of these neurons to other stress-related brain nuclei, such as the paraventricular nucleus, medial amygdala, locus coeruleus and periaqueductal gray, positioning them as a key processing hub in the brain's stress network. Ucn3, the natural primary ligand for CRFR2 in the pBNST, caused enhanced excitability of these neurons by inducing a depolarization, an increase in the input

resistance, and, consequently, increased firing of APs, emphasizing its potential for future drug treatment.

Remarkably, activation and inhibition of pBNST CRFR2 neurons seemed to exert temporally distinct effects, inducing rather immediate, short-lasting anxiolytic effects versus delayed, longer-lasting anxiogenic effects respectively. Although we can only speculate about the potential underlying mechanisms at this point, we expect that these temporal differences arise from differentially modulated synaptic release from the manipulated cells. Silencing the release of GABA and potentially other neuromodulators and neuropeptides at the target sites by photoinhibition could act cumulatively and only take effect much more slowly than directly inducing their release by photoactivation. Alternatively, the vesicle release of neuromodulators by photoactivation could induce a temporary depletion of local vesicle stores, thereby preventing long-lasting effects of activation. As the BNST—and the CRF system within the BNST in particular²⁸—has been suggested to be involved in the modulation of sustained states of anxiety,⁶ suggesting longer-lasting effects of its manipulation, future dedicated studies should target these effects on synaptic transmission at the target sites.

Together, these data provide an important opportunity for pharmacological intervention studies specifically targeting these neurons by means of administration of CRFR2 agonists. However, particular care has to be taken in exploring such interventions,

as many effects of CRFR2 activation have been shown to be dose dependent and cell type specific.^{29,30} In the raphe nucleus, for example, it has been shown that serotonergic neurons are predominantly inhibited by low doses of CRFR2 ligand, whereas they are activated at higher doses through disinhibition, as the majority of non-serotonergic (that is, GABAergic) raphe nucleus neurons are inhibited by such dose.²⁹ Moreover, the effects of CRFR2 activation are brain region specific and depend on previous stress history. For example, in the lateral septum, CRFR2 activation has been related to depressed glutamatergic synaptic transmission, which is switched to facilitation (at a comparable potency) following stress exposure,^{31,32} and local activation of CRFR2-expressing neurons was shown to promote anxious behavior and generate stress-induced behavioral and neuroendocrine dimensions of a persistent anxiety state.³³ Such state- and dose-dependent effects of CRFR2 activation could be expected in the BNST as well, particularly as both anxiogenic¹⁷ and anxiolytic^{18,34} effects of CRFR2 activation have been reported in this region. These findings indicate that there is a strong regional dependency in the effects of activation of CRFR2 neurons, which should be further explored in future studies. Future dedicated studies should therefore investigate this regional dependency of activation of CRFR2-expressing neurons and test under which exact conditions local agonist administration modulates pBNST CRFR2 signaling such that it produces the observed stress-ameliorating effects.

Remarkably, although generally suppressed corticosterone responding has been linked to PTSD pathology,^{17,35} activation of pBNST CRFR2 neurons in this study reduced corticosterone responses to stress and the risk of PTSD. These effects were even correlated, as in the latter experiment stress-induced corticosterone levels positively predicted PTSD symptom scores ($\rho_{(23)} = 0.423$, $P = 0.044$, Supplementary Figure 11), indicating a seemingly protective effect of low corticosterone responses. Many contradictory findings have been reported on the association between HPA axis responsivity and PTSD in both human literature and literature on animal models for PTSD,^{26,36} which seem to be related to either differential assessment of HPA axis reactivity (for example, by means of pharmacological and non-pharmacological challenges),³⁶ or the exact environmental settings (for example, the intensity of the trauma, delay to the subsequent stressor, its nature and duration).³⁷ Therefore, the relatively stressful history of our animals (including surgery and repeated handling) may be related to these contrasting findings. Future work should aim at elucidating the complex association between corticosterone signaling and PTSD.

Finally, our findings propose CRFR2 neurons in the pBNST as an important, yet understudied, node in the brain circuitry regulating stress response and recovery. Future studies should explore the exact neural circuitries involved to identify new potential routes for therapeutic intervention in stress-related disorders.

CONFLICT OF INTEREST

The authors declare no conflict of interest.

ACKNOWLEDGMENTS

We thank S Ovadia for his devoted assistance with animal care. We thank A Ramot and D Harbich for their technical assistance. M Henckens is the recipient of the Niels Stensen Fellowship and a Dean of Faculty Postdoctoral Fellowship of the Feinberg Graduate School of the Weizmann Institute of Science. O Yizhar is supported by the Israel Science Foundation (1351/12), the European Research Council (337637) and Marie Curie CIG (321919). A Chen is the head of the Max Planck Society—Weizmann Institute of Science Laboratory for Experimental Neuropsychiatry and Behavioral Neurogenetics. His work is supported by: an FP7 grant from the European Research Council (260463); research grant from the Israel Science Foundation (1565/15); the Max Planck Foundation; a research support from Roberto and Renata Ruhman; Bruno and Simone Licht; Estate of Toby Bieber; the Henry

Chanoch Krentler Institute for Biomedical Imaging and Genomics; the Perlman Family Foundation, Founded by Louis L and Anita M Perlman; the Adelis Foundation and the Irving I Moskowitz Foundation; I-CORE Program of the Planning and Budgeting Committee and the Israel Science Foundation (grant no. 1916/12).

AUTHOR CONTRIBUTIONS

MJAGH, YP, US, JD, ML, YD, CK and AK conducted the experiments. NJJ provided mice. ME, JMD, OY and AC supervised experiments. MJAGH, YP, JD, JMD, NJJ, OY and AC wrote the manuscript.

REFERENCES

- Herman JP, Ostrander MM, Mueller NK, Figueiredo H. Limbic system mechanisms of stress regulation: hypothalamo-pituitary-adrenocortical axis. *Prog Neuro-psychopharmacol Biol Psychiatry* 2005; **29**: 1201–1213.
- Avery SN, Claus JA, Winder DG, Woodward N, Heckers S, Blackford JU. BNST neurocircuitry in humans. *NeuroImage* 2014; **91**: 311–323.
- Myers B, Dolgas CM, Kasckow J, Cullinan WE, Herman JP. Central stress-integrative circuits: forebrain glutamatergic and GABAergic projections to the dorsomedial hypothalamus, medial preoptic area, and bed nucleus of the stria terminalis. *Brain Struct Funct* 2014; **219**: 1287–1303.
- Lebow MA, Chen A. Overshadowed by the amygdala: the bed nucleus of the stria terminalis emerges as key to psychiatric disorders. *Mol Psychiatry* 2016; **21**: 450–463.
- Choi DC, Furay AR, Evanson NK, Ostrander MM, Ulrich-Lai YM, Herman JP. Bed nucleus of the stria terminalis subregions differentially regulate hypothalamic-pituitary-adrenal axis activity: implications for the integration of limbic inputs. *J Neurosci* 2007; **27**: 2025–2034.
- Davis M, Walker DL, Miles L, Grillon C. Phasic vs sustained fear in rats and humans: role of the extended amygdala in fear vs anxiety. *Neuropsychopharmacology* 2010; **35**: 105–135.
- Dong HW, Swanson LW. Organization of axonal projections from the anterolateral area of the bed nuclei of the stria terminalis. *J Comp Neurol* 2014; **468**: 277–298.
- Dong HW, Swanson LW. Projections from bed nuclei of the stria terminalis, posterior division: implications for cerebral hemisphere regulation of defensive and reproductive behaviors. *J Comp Neurol* 2004; **471**: 396–433.
- Dong HW, Swanson LW. Projections from bed nuclei of the stria terminalis, dorso-medial nucleus: implications for cerebral hemisphere integration of neuroendocrine, autonomic, and drinking responses. *J Comp Neurol* 2006; **494**: 75–107.
- Dong HW, Swanson LW. Projections from bed nuclei of the stria terminalis, magnocellular nucleus: implications for cerebral hemisphere regulation of micturition, defecation, and penile erection. *J Comp Neurol* 2006; **494**: 108–141.
- Boudaba C, Szabó K, Tasker JG. Physiological mapping of local inhibitory inputs to the hypothalamic paraventricular nucleus. *J Neurosci* 1996; **16**: 7151–7160.
- van Pett K, Viau V, Bittencourt JC, Chan RK, Li HY, Arias C *et al*. Distribution of mRNAs encoding CRF receptors in brain and pituitary of rat and mouse. *J Comp Neurol* 2000; **428**: 191–212.
- Bale TL, Contarino A, Smith GW, Chan R, Gold LH, Sawchenko PE *et al*. Mice deficient for corticotropin-releasing hormone receptor-2 display anxiety-like behaviour and are hypersensitive to stress. *Nat Genet* 2000; **24**: 410–414.
- Coste SC, Kesterson RA, Heldwein KA, Stevens SL, Heard AD, Hollis JH *et al*. Abnormal adaptations to stress and impaired cardiovascular function in mice lacking corticotropin-releasing hormone receptor-2. *Nat Genet* 2000; **24**: 403–409.
- Kishimoto T, Radulovic J, Radulovic M, Lin CR, Schrick C, Hooshmand F *et al*. Deletion of *chr2* reveals an anxiolytic role for corticotropin-releasing hormone receptor-2. *Nat Genet* 2000; **24**: 415–419.
- Neufeld-Cohen A, Tsoory MM, Evans AK, Getselter D, Gil S, Lowry CA *et al*. A triple urocortin knockout mouse model reveals an essential role for urocortins in stress recovery. *Proc Natl Acad Sci USA* 2010; **107**: 19020–19025.
- Lebow M, Neufeld-Cohen A, Kuperman Y, Tsoory M, Gil S, Chen A. Susceptibility to PTSD-like behavior is mediated by corticotropin-releasing factor receptor type 2 levels in the bed nucleus of the stria terminalis. *J Neurosci* 2012; **32**: 6906–6916.
- Elharrar E, Warhaftig G, Issler O, Sztainberg Y, Dikshtein Y, Zahut R *et al*. Over-expression of corticotropin-releasing factor receptor type 2 in the bed nucleus of stria terminalis improves posttraumatic stress disorder-like symptoms in a model of incubation of fear. *Biol Psychiatry* 2013; **74**: 827–836.
- Liu P, Jenkins NA, Copeland NG. A highly efficient recombinase-based method for generating conditional knockout mutations. *Genome Res* 2003; **13**: 476–484.
- Tye KM, Prakash R, Kim SY, Fenno LE, Grosenick L, Zarabi H *et al*. Amygdala circuitry mediating reversible and bidirectional control of anxiety. *Nature* 2011; **471**: 358–362.
- Barnard GA. A new test for 2×2 tables. *Nature* 1945; **156**: 177.
- Li C, Vaughan J, Sawchenko PE, Vale WW. Urocortin III-immunoreactive projections in rat brain: partial overlap with sites of type 2 corticotropin-releasing factor receptor expression. *J Neurosci* 2002; **22**: 991–1001.

- 23 Carola V, D'Olimpio F, Brunamonti E, Mangia F, Renzi P. Evaluation of the elevated plus-maze and open-field tests for the assessment of anxiety-related behaviour in inbred mice. *Behav Brain Res* 2002; **134**: 49–57.
- 24 Koch M. The neurobiology of startle. *Prog Neurobiol* 1999; **59**: 107–128.
- 25 Holmes A, Singewald N. Individual differences in recovery from traumatic fear. *Trends Neurosci* 2013; **36**: 23–31.
- 26 Jennings JH, Sparta DR, Stamatakis AM, Ung RL, Pleil KE, Kash TL *et al*. Distinct extended amygdala circuits for divergent motivational states. *Nature* 2013; **496**: 224–228.
- 27 Kim SY, Adhikari A, Lee SY, Marshel JH, Kim CK, Mallory CS *et al*. Diverging neural pathways assemble a behavioural state from separable features in anxiety. *Nature* 2013; **496**: 219–223.
- 28 Walker DL, Miles LA, Davis M. Selective participation of the bed nucleus of the stria terminalis and CRF in sustained anxiety-like versus phasic fear-like responses. *Prog Neuropsychopharmacol Biol Psychiatry* 2009; **33**: 1291–1308.
- 29 Liu J, Yu B, Neugebauer V, Grigoriadis DE, Rivier J, Vale WW *et al*. Corticotropin-releasing factor and urocortin 1 modulate excitatory glutamatergic synaptic transmission. *J Neurosci* 2004; **24**: 4020–4029.
- 30 Pemar L, Curtis AL, Vale WW, Rivier JE, Valentino RJ. Selective activation of corticotrophin-releasing factor 2 receptors on neurochemically identified neurons in the rat dorsal raphe nucleus reveals dual actions. *J Neurosci* 2004; **24**: 1305–1311.
- 31 Liu J, Yu B, Orozco-Cabal L, Grigoriadis DE, Rivier J, Vale WW *et al*. Chronic cocaine administration switches corticotropin-releasing factor2 receptor-mediated depression to facilitation of glutamatergic transmission in the lateral septum. *J Neurosci* 2005; **25**: 577–583.
- 32 Gallagher JP, Orozco-Cabal LF, Liu J, Shinnick-Gallagher P. Synaptic physiology of central CRH system. *Eur J Pharmacol* 2008; **583**: 215–225.
- 33 Anthony TE, Dee N, Bernard A, Lerchner W, Heintz N, Anderson DJ. Control of stress-induced persistent anxiety by an extra-amygdala septohypothalamic circuit. *Cell* 2014; **156**: 522–536.
- 34 Greenberg GD, Howerton CL, Trainor BC. Fighting in the home cage: agonistic encounters and effects on neurobiological markers within the social decision-making network of house mice (*Mus musculus*). *Neurosci Lett* 2014; **566**: 151–155.
- 35 Daskalakis NP, Lehrner A, Yehuda R. Endocrine aspects of post-traumatic stress disorder and implications for diagnosis and treatment. *Endocrinol Metab Clin North Am* 2013; **42**: 503–513.
- 36 de Kloet CS, Vermetten E, Geuze E, Kavelaars A, Heijnen CJ, Westenberg HG. Assessment of HPA-axis function in posttraumatic stress disorder: pharmacological and non-pharmacological challenge tests, a review. *J Psychiatr Res* 2006; **40**: 550–567.
- 37 Belda X, Fuentes S, Daviu N, Nadal R, Armario A. Stress-induced sensitization: the hypothalamic-pituitary-adrenal axis and beyond. *Stress* 2015; **18**: 269–279.



This work is licensed under a Creative Commons Attribution-NonCommercial-NoDerivs 4.0 International License. The images or other third party material in this article are included in the article's Creative Commons license, unless indicated otherwise in the credit line; if the material is not included under the Creative Commons license, users will need to obtain permission from the license holder to reproduce the material. To view a copy of this license, visit <http://creativecommons.org/licenses/by-nc-nd/4.0/>

© The Author(s) 2016

Supplementary Information accompanies the paper on the Molecular Psychiatry website (<http://www.nature.com/mp>)